

UNIVERSITY OF
CALIFORNIA

Ernest O. Lawrence

*Radiation
Laboratory*

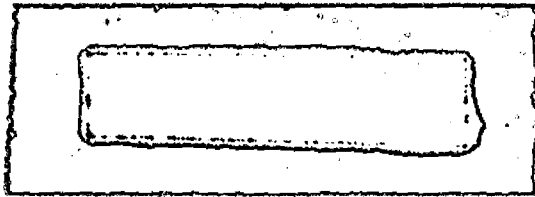
TWO-WEEK LOAN COPY

*This is a Library Circulating Copy
which may be borrowed for two weeks.
For a personal retention copy, call
Tech. Info. Division, Ext. 5545*

BERKELEY, CALIFORNIA

DISCLAIMER

This document was prepared as an account of work sponsored by the United States Government. While this document is believed to contain correct information, neither the United States Government nor any agency thereof, nor the Regents of the University of California, nor any of their employees, makes any warranty, express or implied, or assumes any legal responsibility for the accuracy, completeness, or usefulness of any information, apparatus, product, or process disclosed, or represents that its use would not infringe privately owned rights. Reference herein to any specific commercial product, process, or service by its trade name, trademark, manufacturer, or otherwise, does not necessarily constitute or imply its endorsement, recommendation, or favoring by the United States Government or any agency thereof, or the Regents of the University of California. The views and opinions of authors expressed herein do not necessarily state or reflect those of the United States Government or any agency thereof or the Regents of the University of California.



UCRL-9554

UNIVERSITY OF CALIFORNIA
Lawrence Radiation Laboratory
Berkeley, California

Contract No. W-7405-eng-48

RECOIL-FREE RESONANT ABSORPTION IN Au¹⁹⁷

D. A. Shirley, M. Kaplan, and P. Axel

February 5, 1961

RECOIL-FREE RESONANT ABSORPTION IN Au¹⁹⁷

D. A. Shirley and M. Kaplan

Lawrence Radiation Laboratory and Department of Chemistry
University of California, Berkeley, California

and

P. Axel

Physics Department, University of Illinois, Urbana, Illinois

ABSTRACT

The Mössbauer absorption in Au has been measured at 4°K for the 77-kev gamma ray emitted by Au¹⁹⁷ nuclei embedded in gold, platinum, stainless steel iron, cobalt, and nickel. In each case, a Doppler-shift curve was measured to find the effective width and the chemical shift as well as the amount of resonant recoil-free absorption. The recoil-free fractions, f , are obtained with the aid of a straightforward analysis, which incidentally shows the errors that can be made in f if the chemical shift and effective width are not taken into account.

The observed recoil-free emission fractions were found to be approximately 0.06(Au), 0.34 and 0.14 (Pt), 0.24 (steel), 0.32 (Fe), 0.27 (Co), and 0.35 (Ni). The relative f values are correct, independent of possible errors in the parameters of the single absorber that was used. If extreme assumptions are made, the absolute f values might require a multiplicative correction factor that could be as small as 0.53.

Relatively large f values were obtained when the Au¹⁹⁷ radioactive nuclei were in high Debye-temperature lattices composed of light nuclei. Particularly low f values were found when the largest radiation-damage effects were expected.

The observed chemical shifts were (in units of 10^{-6} ev) $< 0.13, 0.26, 1.3, 1.4, 1.3,$ and 1.1 for gold, platinum, steel, iron, cobalt, and nickel, respectively. These chemical shifts give information more directly interpretable than, but related to, the optical-isotope and isomer shifts, and the Knight shift. If the nuclear-charge radius of the excited state of Au^{197} is smaller than that of the ground state, the magnitudes of the shifts measure directly the depletion of electron density at the radioactive nuclei in the different lattices.

Zeeman splittings of the nuclear energy levels caused by local magnetic fields at Au had relative magnitudes of $1.0: 0.43: < 0.10$ for Fe, Co, and Ni lattices. If the magnetic moment of the 77-kev excited state in Au^{197} is 1.6 nm , the local magnetic fields in Fe and Co were 282 and 122 koe, respectively.

RECOIL-FREE RESONANT ABSORPTION IN Au^{197*}

D. A. Shirley and M. Kaplan

Lawrence Radiation Laboratory and Department of Chemistry
University of California, Berkeley, California

and

P. Axel[†]

Physics Department, University of Illinois, Urbana, Illinois

February 5, 1961

I. INTRODUCTION

This paper presents the results of a series of experiments which exploit the sensitivity of the Mössbauer effect¹ to energy changes produced by the environment of atomic nuclei. These results are based on the observed recoil-free resonant absorption by Au¹⁹⁷ nuclei of the 77-keV de-excitation gamma ray from the first excited state of Au¹⁹⁷. Both the negative beta-ray parent, Pt¹⁹⁷, and the K-capture parent, Hg¹⁹⁷, were used in different host materials as sources. The following four quantities have been measured for eight different combinations of source and absorber:

- (a) the energy width of the observed resonance,
- (b) the fraction of events that gave recoil-free resonant absorption,
- (c) the chemical-energy shifts produced by the different coulomb-interaction energies of the nuclear-charge distributions (of the ground and excited states of Au¹⁹⁷ nuclei) with the different electron densities characteristic of the different environments,
- (d) the hyperfine structure which was apparent due to the strong local magnetic fields at the Au nuclei when they were embedded in hosts of metallic iron or cobalt.

Our measurements have disclosed several interesting effects. In particular, these are the first experimental results that show (a) that heavy nuclei in a host material of light atoms can produce large recoil-free effects (as might be implied by the Debye temperature of the host material) and (b) that nuclear states corresponding to different proton orbitals produce particularly large chemical shifts.

The apparent width of a resonance is quite important in determining the fraction of recoil-free events, f . In cases in which f values have been inferred from experimental data without due regard for the apparent width, these inferred f values are lower limits of the true f values. Until the mechanism of line broadening is understood in detail, complete Doppler shift curves will be needed to deduce f values. A final interesting effect is the improvement in the precise determination of absorber parameters that can be attained if identical source and absorber can be used.

II. ANALYSIS OF A DOPPLER-SHIFT MÖSSBAUER EXPERIMENT

A. Complexity Introduced by Finite Absorber Thickness

Thick absorbers introduce into Mössbauer experiments the mathematical complexity typical of significant energy-dependent absorption. An absorber consisting of n atoms/cm² each of which has an absorption cross section, $\sigma(E)$, transmits a fraction $T(E)$ of the incident photons (or particles), where

$$T(E) = \exp[-n \sigma(E)] . \quad (1)$$

If the incoming beam has an energy distribution $N(E) dE$, the transmitted beam has an altered energy distribution, $[N(E)]_T dE$.

Frequently the absorption parameters can be determined most easily by studying the total absorption, A , that occurs as E is varied over the entire range in which $\sigma(E)$ is significantly large. The absorption, A , is represented by the area under a transmission curve:

$$A = \frac{\int_0^{\infty} N(E) dE - \int_0^{\infty} [N(E)]_T dE}{\int_0^{\infty} N(E) dE} . \quad (2)$$

Measured A values are particularly important because it is often difficult to measure $[N(E)]_T$ directly (e. g., because of resolution or thermal-velocity broadening).

The familiar Lorentz form often is an adequate representation of $\sigma(E)$:

$$\sigma(E) = \frac{\sigma_m'}{\left[\frac{2}{\Gamma'} (E - E_0') \right]^2 + 1} , \quad (3)$$

where σ_m' is the effective maximum cross section, and Γ' is the full width at half maximum. For example, the resonant absorption of neutrons, as given by the Breit-Wigner formula,² follows this energy dependence. The

analysis of early experiments with slow neutrons discussed the absorption implied by Eqs. (1) through (3) as well as the additional complications introduced into neutron experiments by the thermal velocities of the absorbing nuclei.^{3,4} In addition to the early calculations,⁴ more extensive numerical results were obtained,^{5,6} and convenient summaries of these exist.⁷ (Of course, the calculations given as a function of the thermal velocity parameter, Δ , can be adapted simply to Eq. (3) by setting $\Delta = 0$.)

Although these analyses (designed for resonant neutron absorption experiments) could be used to help interpret the data obtained in Mössbauer experiments, there are special features of the Mössbauer experiment which make a somewhat different approach more convenient. In particular, a Doppler-shift Mössbauer experiment makes it quite easy to measure the absorption as a function of energy, i. e., $\{N(E) - [N(E)]_T\} / N(E)$. The specific analysis given below is designed to show explicitly the relation between the experimental data and both the recoil-free fractions and the various line widths that enter into the problem.

B. Standard Analysis Applicable to Finite Absorber Thickness

In the typical Mössbauer Doppler-shift experiment, a detector beyond the absorber counts N_0 gamma rays when conditions (such as very rapid Doppler velocities or very high temperatures) make nuclear resonant absorption impossible. A fraction $(1-f)$ of these gamma rays have the wrong energy to be absorbed resonantly at experimentally achievable Doppler velocities. (These $(1-f)N_0$ gamma rays may have received large energy shifts because of nuclear recoil at emission, or they may be gamma rays of a quite different energy unresolved by the detector from gamma rays of interest. Whenever possible, the effect of gamma rays of different energy is subtracted so that the f values usually quoted are the fraction of gamma rays of one nominal energy, E_0 , that are recoil-free.)

It is customary^{8, 9, 10} to consider first the case in which the fN_0 recoil-free gamma rays have Lorentz distributions with the same width, Γ' . Their energy distribution is

$$N(E)dE = f \frac{N_0}{\pi} \frac{\frac{2}{\Gamma'} dE}{\left[\frac{2}{\Gamma'} (E-E_0) \right]^2 + 1} = f \frac{N_0}{\pi} \frac{dy}{y^2 + 1}, \quad (4)$$

where $y \equiv 2(E-E_0) / \Gamma'$ and where E_0 will be different from E_0' of Eq.(3) if there is a chemical shift. Note that $N(E)$ in Eq. (4) has been normalized to $f N_0$:

$$\int_0^{\infty} N(E)dE = 2 \int_{-\infty}^{\infty} N(y)dy = 2 \int_0^{\infty} N(y)dy = f N_0. \quad (5)$$

Defining the chemical-shift parameter, c , by $c \equiv 2(E_0 - E_0') / \Gamma'$ gives:

$$\sigma(E) = \frac{\sigma_m'}{(y+c)^2 + 1}. \quad (6)$$

The introduction of c is the obvious generalization of the standard treatment to include chemical shifts. If a Doppler-shift curve is measured, the presence of a finite c can be taken into account trivially. However, c should be known before interpreting either data taken at zero Doppler velocity or data taken combining measurements appropriate to $+v$ and $-v$.

A Doppler-shift curve is obtained by increasing the relative distance between source and absorber at a rate given by the relative velocity, $+v$. For a given velocity v , the emitted gamma-ray energy E that experiences the cross section σ_m' is $E = E_0' + v/c E_0$. The cross section appropriate to E then depends on v . Defining $u = (2vE_0) / (\Gamma'c)$, this cross section can be expressed in terms of dimensionless variables as

$$\sigma(y, u) = \frac{\sigma_m'}{(y+c-u)^2 + 1}. \quad (7)$$

The absorber consists of n atoms/cm² of the correct isotope (in the correct hyperfine state if there is significant hyperfine splitting). However, only a fraction f' of these atoms can absorb a photon of energy near E_0 without recoil; therefore, only nf' atoms have the effective cross section given in Eq. (7). It is convenient to characterize the absorber thickness by t , which is the number of absorption lengths of the absorber for a gamma ray that is exactly resonant (i. e., $t = n f' \sigma_m'$).

Let $N(n, u)$ or $N(t, u)$ be the total number of gamma rays counted by the detector when the relative velocity is v . Then we can write

$$N(n, u) = (1-f)N_0 + f \frac{N_0}{\pi} \int_{-\infty}^{\infty} \frac{dy}{1+y^2} \exp[-nf' \sigma(y, u)] \quad (8)$$

$$N(t, u) = (1-f)N_0 + f \frac{N_0}{\pi} \int_{-\infty}^{\infty} \frac{dy}{1+y^2} \exp\{-t[(y+c-u)^2 + 1]^{-1}\} \quad (9)$$

When $u = c$, the integral in Eq. (6) can be evaluated analytically:⁴

$$N(t, c) = (1-f)N_0 + f N_0 e^{-t/2} J_0\left(\frac{it}{2}\right) \quad (10)$$

where $J_0\left(\frac{it}{2}\right) = I_0(t/2)$ is the zero-order Bessel function of imaginary argument evaluated at $t/2$.

Although $N(t, u)$ has not been expressed analytically, numerical calculations have shown⁸ that, for $t < 10$, $[N_0 - N(t, u)]$ is approximately a Lorentz line with an apparent width, Γ_a :⁸

$$[N_0 - N(t, u)] = \frac{N_0 - N(t, c)}{\left(\frac{u\Gamma'}{\Gamma_a}\right)^2 + 1} = \frac{fN_0 \left[1 - e^{-t/2} J_0\left(\frac{it}{2}\right)\right]}{(u\Gamma'/\Gamma_a)^2 + 1}, \quad (11)$$

where Γ_a increases with t . It is convenient to define the line-broadening function $h(t)$ by:

$$\Gamma_a = 2\Gamma' h(t). \quad (12)$$

From his numerical calculations, Visscher gives:⁸

$$h(t) = 1 + 0.135t \quad \text{for } 0 \leq t \leq 5 \quad (13a)$$

$$h(t) = (1 + 0.145t - 0.0025t^2) \quad \text{for } 4 \leq t \leq 10. \quad (13b)$$

Identical values of $h(t)$ have been found for very thin sources by Margulies and Ehrman who have also calculated $h(t)$ for sources of finite thickness.¹¹

A method that has been used for finding f and f' involves first trying to find f and t from the equation:

$$\frac{N_0 - N(t, c)}{N_0} = \frac{N(t, \infty) - N(t, c)}{N(t, \infty)} = f \left[1 - e^{-t/2} I_0 \left(\frac{t}{2} \right) \right] = f p(t) \quad (14)$$

where

$$p(t) \equiv \left[1 - e^{-t/2} I_0 \left(\frac{t}{2} \right) \right]. \quad (15)$$

For example, t has been inferred from Eq. (14) by matching the data obtained with a series of absorbers and a single source. However, because $p(t)$ does not vary rapidly with t , this procedure does not give very precise t values. Furthermore, the assumed proportionality between $t = n \sigma_m' f'$ and n is correct only if neither σ_m' nor f' change. In view of the dependence of σ_m' both on Γ' (to be discussed below) and on f' , some effort should be made to control or to check on the constancy of Γ' and f' . One obvious procedure (which has not been reported explicitly) would entail obtaining a series of nearly identical thin absorbers and stacking these to obtain larger thicknesses. (The individual foils could be used independently in order to verify their identity, which is so crucial to the analysis.)

C. Determination of f' : value of σ_m'

Once t has been determined for a given absorber, the product $\sigma_m' f'$ is known. However, only an upper limit for σ_m' can be calculated from the known properties of the excited nuclear state.

A fundamental quantum-mechanical property of photons is that if a quantum-mechanical state has a total width equal to its width for photon emission, the absorption cross section at resonance is $2\pi \lambda^2 (2I_{ex} + 1)/(2I_g + 1)$. It is also relatively well known that if the state has any other mode of decay, the absorption at resonance decreases by the factor Γ_γ/Γ , where Γ is the total level width. For example, Jackson¹² has emphasized that when only internal conversion competes with gamma-ray emission, the maximum cross section, σ_m becomes^{12'}

$$\sigma_m = 2\pi \lambda^2 \frac{(2I_{ex} + 1)}{(2I_g + 1)} \frac{1}{(1 + \alpha)}, \quad (16)$$

where α is the total internal-conversion coefficient, N_e/N_γ . Thus, if the absorption cross section is characterized by a Lorentz-shaped parameter Γ' , we have

$$\sigma_m' = 2\pi \lambda^2 \frac{(2I_{ex} + 1)}{(2I_g + 1)} \frac{\Gamma_\gamma}{\Gamma'} \quad (17a)$$

If only internal conversion competes with photon emission we have

$\Gamma = (1 + \alpha) \Gamma_\gamma$, and σ_m' becomes

$$\sigma_m' = \sigma_m \Gamma/\Gamma' \quad (17b)$$

The validity of Eq. (17b) can be established simply by considering the actual absorption to be caused by nuclei that all have the natural width, Γ , but have different resonant energies, E_0 . The total area under an absorption-cross-section curve representing the total effect of n atoms, is $n\pi\Gamma\sigma_m/2$, where σ_m is given by Eq. (16). If the total-cross-section curve can also be represented as a Lorentz curve with σ_m' and Γ' , this same area is $n\pi\Gamma'\sigma_m'/2$. It is perhaps ironic that Jackson is sometimes quoted as the authority for using Eq. (16) rather than Eq. (17b) as the value of σ_m' , because the omission of Γ/Γ' is analogous to the omission of Γ_γ/Γ , which was being corrected by Jackson.¹²

These considerations make it clear that those values of f' inferred with the aid of Eq. (16) despite a known difference between Γ' and Γ should be corrected upward by a factor of Γ'/Γ . Furthermore, although other f' values that were calculated by assuming $\Gamma' = \Gamma$ may be correct, they might more properly be treated as lower limits of f' until line broadening is better understood.

Equation (17a) implies that σ_m' can be evaluated even if the total conversion coefficient is unknown provided only that Γ_γ is known. For example, coulomb-excitation data often give Γ_γ directly. If the gamma-ray multipolarity is mixed, the mixing (as implied by relative internal-conversion coefficients for different electronic shells or subshells) can be used to find the total Γ_γ from the partial electric width obtained from coulomb-excitation experiments.

D. Determination of Γ'

If one had a source and an absorber which were both characterized by Lorentz lines of the same width, Γ' , a measurement of the experimental Doppler-curve width, Γ_a , could be used (together with an experimentally determined value of t) to find Γ' with the aid of Eqs. (12) and (13). However, these equations are valid only if the width characteristic of the source, $(\Gamma')_s$ is equal to the absorber width, Γ' . Furthermore, the Doppler absorption curve can be approximately Lorentzian without implying that $(\Gamma')_s = \Gamma'$. For example, for a range of $(\Gamma')_s$ near Γ' , Eq. (12) is probably changed only in that $2\Gamma'$ is replaced by $[\Gamma' + (\Gamma')_s]$. Equation (10) would probably have a similar form, but Eqs. (11) and (14) would change because the peak absorption would be different. Another simple situation in which a Doppler curve would be Lorentzian is the case for $(\Gamma')_s \ll \Gamma'$. In fact, if $N(E) dE$ has a very small energy spread, it need not have a Lorentzian form to give a Lorentzian Doppler curve. (Of course, if the absorption cross section, $\sigma(E)$, were not a Lorentz curve as given by Eq. (3), Eq. (8) would have to be reevaluated to find replacements for Eqs. (10) through (14).

The only simple unambiguous situation is one in which the natural width Γ is known and in which the observed Γ_a implies $\Gamma' = (\Gamma')_s = \Gamma$. If this condition does not hold, one may be able to draw plausible inferences about Γ' from measurements with several different sources and several different absorbers. However, such inferences will remain in doubt until one understands better the factors that enlarge Γ' . On the brighter side, as will be shown below, some data can be interpreted even if Γ' is unknown.

In the experimental work described below, we have attempted to determine Γ' by using identical gold foils as source and absorber in the hope that this would assure the equality of $(\Gamma')_s$ and Γ' . This procedure has the

very important advantage of quite possibly producing equal recoil-free fractions f and f' in the source and absorber.

E. Determination of f and f' : area method

Consider first the absorption area under the normalized Doppler-shift curve when $(\Gamma')_s = \Gamma'$:

$$(\text{Area})_d = \int_{-\infty}^{+\infty} du \frac{N(t, \infty) - N(t, u)}{N(t, \infty)} = \int_{-\infty}^{+\infty} du \frac{f p(t)}{\left(\frac{u\Gamma'}{\Gamma_a}\right)^2 + 1} \quad (18)$$

or

$$(\text{Area})_d = \pi \frac{\Gamma_a}{\Gamma'} f p(t) = 2\pi h(t) f p(t). \quad (19)$$

The subscript d is used as a reminder that Eq. (19) applies to the dimensionless area obtained when the absorption is plotted as a function of the dimensionless variable, $u = (2vE_0/\Gamma'c)$. To obtain the area under an absorption-vs-velocity curve, Eq. (19) should be multiplied by $(\Gamma'c/2E_0)$ to give

$$\text{Area} = \pi \frac{c}{E_0} \Gamma' f h(t) p(t). \quad (20a)$$

Equation (20a), which seems to imply that t and Γ' must be known to derive f from a measured area, is somewhat misleading because of the obscurity of the implicit dependence of t on Γ' and f' . Equations that are more informative in many circumstances can be obtained by approximating $h(t) p(t)$ and by substituting $n \sigma_m f' \Gamma/\Gamma'$ for t . For small t , we can write

$$\text{Area} = \frac{\pi}{2} \frac{c}{E_0} n \sigma_m \Gamma f f' (1 - 0.24t + 0.04t^2). \quad (20b)$$

Equation (20b) is accurate to within 3% for $t \leq 2$; the area given should be reduced by 7% for $t = 3$, and by 22% for $t = 4$. For $4 \leq t \leq 10$, to better than 3%, we have

$$\text{Area} = \frac{1.2\pi}{2} \frac{c}{E_0} \Gamma' f [1 + 0.20t] \quad (20c)$$

or

$$\text{Area} = \frac{1.2\pi}{2} \frac{c}{E_0} f(\Gamma' + 0.20n\sigma_m \Gamma' f'), \quad (20d)$$

where the second term in brackets is twice as large as the first when $t = 10$. Equations (20b) and (20c) are equal at $t = 3$.

Although Eq. (20) was derived for $(\Gamma')_s = \Gamma'$, it applies equally well for an arbitrary $N(E)dE$ emitted from a source. [Only for $(\Gamma')_s = \Gamma'$ do we have $\Gamma_a = 2\Gamma' h(t)$; therefore, only in this case can Γ' be determined directly from Γ_a and t .] The universal applicability of Eq. (20) can be seen easily by considering a photon of arbitrary energy, E' (near E_0 or E_0'). During a complete Doppler-shift experiment, as v varies, this photon experiences every possible value of transmission:

$\exp(-t/\{1 + [2(E' - E_0' - \frac{v}{c} E_0)/\Gamma']^2\})$. Therefore, each photon of energy E' contributes the same area to the absorption curve as does any other photon in the energy range swept through resonance during the Doppler shift experiment.

Equation (20b) makes it clear that f for a source could be determined rather precisely if f' for a thin absorber were known, even though Γ' is not known precisely. (For example, f' might be determined directly in a recoil-free Rayleigh-scattering experiment.¹³) On the other hand, if f' is not known, thin-absorber experiments may determine (ff') and t , but they will not give f' and f individually unless Γ' is known.

When an experimental Doppler curve is Lorentzian with full width at half maximum, Γ_{exp} , and with peak absorption, p_{exp} , its area is $\pi c \Gamma_{\text{exp}} p_{\text{exp}} / 2 E_0$. This value substituted into Eq. (20) gives

$$P_{\text{exp}} = \frac{2\Gamma' h(t)}{\Gamma_{\text{exp}}} \quad f p(t) = \frac{\Gamma_a}{\Gamma_{\text{exp}}} f p(t). \quad (21a)$$

For small t , we have

$$P_{\text{exp}} = n \sigma_m \frac{\Gamma}{\Gamma_{\text{exp}}} f f' [1 - 0.24t + 0.04t^2]. \quad (21b)$$

For $4 < t < 10$, we have

$$P_{\text{exp}} = 1.2 \frac{\Gamma'}{\Gamma_{\text{exp}}} f (1 + 0.20t) \quad (21c)$$

$$= 1.2 f \left[\frac{\Gamma'}{\Gamma_{\text{exp}}} + 0.20 n \sigma_m f' \frac{\Gamma}{\Gamma_{\text{exp}}} \right].$$

In the remainder of the paper we shall use Γ_{exp} or Γ_e to signify an experimentally measured width. We reserve Γ_a for the width one would get when $(\Gamma')_s$ equals Γ' and Γ_a is given by Eq. (12).

Although Eqs. (20b), (20c), (21b), and (21c) give helpful insights into the interdependence of the different parameters, Eqs. (20a) and (21a) are as simple as any for the interpretation of most data. Both $p(t)$ and $h(t)$ are very slowly varying functions which can be arranged in easily usable graphical form. Furthermore, the successive approximations often needed to solve these primary equations converge rapidly.

III. DECAY SCHEMES OF Pt¹⁹⁷ AND Hg¹⁹⁷

Both Pt¹⁹⁷ and Hg¹⁹⁷ were used as sources of the 77-keV gamma rays which are emitted during the deexcitation of the first excited state of Au¹⁹⁷. The relevant decay schemes are shown on the energy-level diagram of Fig. 1 mainly as an indication of the radiations that were present.¹⁴ Inasmuch as our sources often contained other radioactive isotopes, any necessary corrections for radioactive decay or for other radiations in the source were based on experimental data obtained with the particular source.

Of the two sources, 18-hr Pt¹⁹⁷ is easier to use because it gives a particularly simple photon spectrum consisting mainly of 77-keV gamma rays. It contains only a small admixture of 191-keV gamma rays and 67-keV Au x-rays due to the internal conversion of the 191-keV gamma rays. However, if nonisotopically enriched Pt is used, 4.3-day Pt¹⁹³ is a strong contaminant which does contribute x-rays. The 65-hr Hg¹⁹⁷ is a poorer source because of the x-rays arising from K capture.

The following paragraphs summarize the information about three properties of Au¹⁹⁷ which will be used later in this paper. These are the internal-conversion coefficient of the 77-keV gamma ray, the lifetime of the 77-keV state, and the magnetic moments of the ground state and the 77-keV state. While these properties are being given, they will be compared with those predicted by the single-particle model if the shell states $d_{3/2}$ and $s_{1/2}$ are associated with the ground and excited states, respectively. This comparison and state identification will be important later in the paper during the interpretation of chemical shifts.

A. Internal Conversion Coefficient

Because the 77-keV transition is a mixture of M1 and E2 radiations, the conversion coefficient, α , cannot be obtained directly from theory. However, measurements of the relative conversion in the different L subshells can be used^{15, 16} together with the theoretical internal-conversion coefficients^{17, 18} to obtain the fraction of the gamma rays which are E2. This fraction, which is quite sensitively determined by the relative subshell values, is 0.10 ± 0.01 . The resultant L-shell conversion coefficient has added uncertainty because of a difference between the two available theoretical values; the values are 3.2 ± 0.1 ¹⁷ and 3.0 ± 0.1 .¹⁸ We shall use the value $\alpha_L = 3.10 \pm 0.10$. The measured relative values of the L, M-, and N-shell conversion¹⁶ can then be used to obtain a total internal-conversion coefficient, α_T , of 3.96 ± 0.14 . In view of the difficulties inherent in direct measurement, this value is probably more reliable than the lower value that was determined experimentally.¹⁶

B. Lifetime

The measured half life of the 77-keV state is 1.9×10^{-9} sec.¹⁹ This value together with the conversion coefficient and branching ratio mentioned above implies a partial M1-photon half life of 1.05×10^{-8} sec and a partial E2-photon half life of 9.5×10^{-8} sec. Compared with the single-particle proton estimates²⁰ (with a nuclear radius of $R = 1.2 \times 10^{-13} A^{1/3}$), the M1 gamma-ray transition rate is slow by a factor of about 330, whereas the E2 transition rate is fast by a factor of about 50.

C. Spins and Magnetic Moments

The ground-state properties of Au¹⁹⁷ are well-known. The measured value of the spin is 3/2.²¹ The magnetic moment, which has been measured quite precisely by several groups, is 0.14 nuclear magnetons.²² Both of these values are in good agreement with the d_{3/2} state predicted to be low-lying by the single-particle shell model. It is therefore attractive to identify the 77-keV state as the predicted low-lying s_{1/2} state of the shell model; this s_{1/2} state appears as the ground state in both stable $_{81}\text{Tl}^{203}$ and $_{81}\text{Tl}^{205}$.^{21, 22, 23} The experimental evidence for the spin of this excited state is based on a comparison of the measured coulomb-excitation probability^{24, 25} with the E2 gamma-ray transition probability. The most precisely measured B(E2) value²⁵ for excitation is $(0.14^{+0.02}_{-0.04}) \times 10^{-48} \text{ cm}^2$ compared with 0.11×10^{-48} or $0.22 \times 10^{-48} \text{ cm}^2$ depending on whether the spin of the 77-keV state is 1/2 or 3/2, respectively. [The expected B(E2) values²⁶ are directly proportional to the fraction of the gamma-ray transitions that are E2 and inversely proportional to $(1 + a_T)$]. These data favor a spin of 1/2 even though, as has been pointed out,²⁵ a spin of 3/2 for the 77-keV state cannot be excluded in view of the uncertainties in the total conversion coefficient. Despite this conceivable uncertainty, we shall later use this s_{1/2} assignment for the 77-keV state to estimate both its magnetic moment, μ , and the spatial distribution of the odd proton. We shall use $\mu = 1.6$ nuclear magnetons because it is the experimental value for the ground states of both $_{81}\text{Tl}^{203}$ and $_{81}\text{Tl}^{205}$.^{22, 23}

D. Expected Widths of Doppler Curves

The minimum width of the expected resonance-absorption line can be estimated directly from the known half life, 1.9×10^{-9} sec. The natural line-width is $\Gamma = 2.4 \times 10^{-7}$ ev, and the minimum experimental full width of the Doppler curve at half maximum is $\Gamma_e = 4.8 \times 10^{-7}$ ev if the absorber and source are infinitely thin. An energy shift of 2.4×10^{-7} ev in a 77-kev gamma ray can be produced by a relative velocity between source and absorber of $v = (3 \times 10^{10}) (2.4 \times 10^{-7}) / 7.7 \times 10^4 = 0.093$ cm/sec. The total change in velocity needed to traverse the minimum full width of the experimental curve at half maximum is 0.196 cm/sec. Of course, larger velocity shifts would be needed if the actual widths Γ'_a and $(\Gamma'_a)_s$ were larger than Γ .

E. Earlier Mössbauer Experiments with Au¹⁹⁷

Measurements similar to some of those given below have been reported.²⁷ These earlier measurements will be compared with ours whenever possible in the following sections.

IV. APPARATUS

The equipment used for all of the measurements is shown in Fig. 2. The 77-keV photons emitted by the stationary source, S, passed through a lead collimator C. That part of the photon beam which was not absorbed by the gold absorber, A, impinged on the NaI scintillation detector, D. The secondary 73-keV Pb x-rays originating in the collimator were negligible.

In most of the experiments, the absorber was a 10-mil disc of gold foil which was rotated by a tilted shaft. The gold was held in place by brass ribs and could easily be replaced by a sample of different thickness. The brass ribs did not introduce any error, but they made it inconvenient to get a zero-motion point because all other points properly averaged the small effect of the brass. The shaft was turned by the synchronous motor, M, which was driven at an easily adjustable speed by the audio oscillator. The beam passed through the gold at a radial distance, R, (measured along the gold) from the shaft. As the foil rotated with a frequency, f, the gold atoms at the beam position had a velocity component in the beam direction equal to $2\pi R f \cos \theta$, where $\theta = 8.07$ deg was the angle between the beam direction and the plane of the gold foil. The geometry was always maintained constant so that $R = 2.5$ cm; thus a rotational speed of 20 rpm produced an effective linear speed of 0.74 cm/sec in the beam direction. The finite size of the beam at the gold produced a variation of ± 0.2 cm in R, which resulted in a $\pm 8\%$ velocity change about the nominal value. This finite velocity resolution was negligible when the chemical shifts were small but may have introduced a broadening of about 2% when steel, iron, cobalt, and nickel hosts were used. In the remainder of the paper, we shall report the nominal velocity of the gold absorber relative to the stationary source; a positive velocity implies motion of the absorber away from the source.

During the experiments the absorber, the lower collimator, and the source were all immersed in liquid helium so that their common temperature was 4.2°K .

This simple apparatus functioned reliably and was well-suited to the measurements to be reported. It had the additional advantage of maintaining a constant distance between source and absorber. On the other hand, the apparatus requires a relatively large absorber and would therefore be unsuitable for rare absorber materials. Furthermore, the constant-percentage velocity spread would not be suitable for absorption patterns with complex structure.

The detector used for the quantitative work reported below was a 6-mm NaI scintillation crystal. This crystal could not resolve the 77-keV gamma rays from 67-keV Au x-rays or neighboring x-rays. However, a xenon-filled proportional counter was used to determine the ratio of 77-keV photons to x-rays in each experiment.

V. RESULTS AND DISCUSSION

The experimental data (except for the magnetic effects observed with Fe and Co hosts) are summarized in Table I together with some derived quantities. Each of the eight lines in the table represent a different combination of source and absorber. As will be noted below, six of the entries are averages of at least two independent runs. The following subsections explain the entries and discuss the implications of the data.

A. Sources and Absorbers

The first three columns indicate the Au¹⁹⁷ parent used, the reaction that produced this parent, and the host material, respectively. The fourth column gives the thickness of the gold absorber used. The first four lines (Group A) involve radioactive parents which were produced in situ in the host material. The Hg¹⁹⁷ in Au source of line 1 was used to calibrate the Au absorber as explained below. Three separate experiments were performed with this combination and their results were averaged. The individual experiments were consistent with each other, but the statistics were poor enough so that no attempt was made to determine a line width from each run. Two independent runs were made with the 5-mil Au absorber (line 2), and both gave the same line width. However, background corrections were available for only one run, and it alone was used to measure the amount of resonant absorption. Three independent runs were made with Pt¹⁹⁷ in Pt sources (line 3). All three gave the same line width (to within one half the quoted error), but background corrections were available only for two. The amount of resonant absorption was identical in these two cases. Two runs were made with the Hg¹⁹⁷ in Pt sources (line 4). The line widths differed by 4% while the areas differed by 7%. These differences are well within the expected experimental error.

Neither these sources nor the absorbers received any controlled heat treatment. The Hg¹⁹⁷ parents (line 1 and 4) were too volatile to allow any annealing of the source after the radioactivity had been produced. Crude annealing was attempted with one of the Pt¹⁹⁷ in Pt sources, but this had no apparent effect on the Doppler-shift curve.

The entries on lines 5 - 8 (Group B) represent experiments in which neutron-irradiated Pt (enriched to about 66% in Pt¹⁹⁶) was alloyed with stainless steel, iron, cobalt, or nickel. In each case the host and radioactive material were heated to about 1550°C and the resulting alloy was quenched. There were about 500 host atoms to each Pt atom in these alloys.

The stainless steel (line 5) was used first in order to see whether there would be a significant recoil-free effect; for this purpose it seemed wise to use an iron alloy which would have no complicating local magnetic fields. Two separate runs were tried and each gave non-Lorentzian Doppler curves with full widths at half maximum of about 8Γ . (The natural line width, Γ , is equal to 2.4×10^{-7} ev; an equal energy shift can be produced by a relative velocity of 0.93 mm/sec.) Both experiments gave equal resonant areas. Three Pt¹⁹⁷-in-Fe sources were used and are averaged on line 6. Their line widths could not be determined very well because of hyperfine and other structure, but the lines seemed to have the same width in all three sources. The resonant-absorption effects obtained with these sources were all within 12% of the mean shown on line 6. The entries on lines 7 and 8 each come from a single source.

When the experiments were begun, two 10-mil Au absorbers were prepared from the same sheet of Au foil. They always appeared to give similar results and were used interchangeably without keeping a record of which was being used. These two 10-mil absorbers will be discussed below

as though they were identical. As Table I indicates, most of the experiments were performed with the 10-mil Au absorber. This absorber was not given any special heat treatment even though annealing might have produced a narrower Doppler-shift curve. Not treating this absorber in a special way had the advantage of keeping it as similar as possible to the Hg¹⁹⁷ sources that were produced in similar 10-mil Au foils. (If the absorber and source had been well-annealed and had given the natural line width before irradiation, radiation damage might have created differences between the source and absorber.) The 5-mil Au absorber was not related to the 10-mil Au absorber (i. e., two identical 5-mil Au absorbers were not used together as a 10-mil absorber).

B. Source and Absorber Line Widths, $(\Gamma')_s$ and Γ'

The fifth column of Table I gives the ratio of the observed Doppler line width, Γ_e , to the natural line width, Γ . The minimum possible value is $(\Gamma_e/\Gamma) = 2$. According to Eq. (12), for $(\Gamma')_s = \Gamma'$, $\Gamma_e = 2\Gamma' h(t)$, where $h(t)$ is the broadening factor due to absorber thickness as given in Eq. (13) for a thin source. To proceed, we shall use the reasonable assumption that $(\Gamma_e/h(t)) = \Gamma' / h(t)$.

Consider the 10-mil Au absorber. Independent of $h(t)$, line 4 makes it clear that we have $\Gamma'/\Gamma \leq 3.8$; if the minimum line broadening (consistent with data to be given below) is assumed, this limit is reduced to about $\Gamma'/\Gamma \leq 3.2$. Of course, the minimum value of this ratio is $\Gamma'/\Gamma \geq 1$.

If we use our best values for the 10-mil absorber [$h(t) = 1.17$ and $\Gamma'/\Gamma = 2.8$] the value of $[(\Gamma')_s/\Gamma]$ becomes

$$\frac{(\Gamma')_s}{\Gamma} = \frac{\Gamma_e}{1.17\Gamma} = 2.8 \tag{22}$$

The $(\Gamma')_s/\Gamma$ ratios implied by the data on lines 3 through 8 become 2.8, 1.3, 4.0, 2.7, 3.2, and 2.7. Note that only the Hg^{197} -in-Pt sources implied a source-emission line close to the natural width. Of course, if Γ' equals Γ for the absorber, the above values of $(\Gamma')_s/\Gamma$ would each be increased by the addition of 1.8, if t remained constant. On the other hand, for $\Gamma' = \Gamma$, t would probably increase, thereby increasing $h(t)$ which is 1.17 in Eq. (22). Thus, the correct $(\Gamma')_s/\Gamma$ is probably not as much as 1.8 greater than the values given above even if Γ' is smaller than the 2.8 assumed.

The two experiments (averaged on line 2) which used a 5-mil Au absorber cannot be interpreted unambiguously because we have insufficient evidence about Γ' in this case. If the 5-mil absorber had the same Γ' and f' that characterize the 10-mil absorber, $[(\Gamma')_s/\Gamma]$ for these Pt sources would be 1.3. (It might seem, at first glance, that this 1.3 value is encouragingly close to the 1.3 value obtained with the Hg^{197} in Pt source (line 4). However, we do not understand why the two sources of line 2 and the two of line 4 should give $[(\Gamma')_s/\Gamma] = 1.3$ while the three sources of line 3 all gave $(\Gamma')_s/\Gamma = 2.8$.)

On the other hand, if the 5-mil Au Doppler curve had been narrow because of a smaller value of Γ' , this value of Γ' would have to be known before $(\Gamma')_s$ could be deduced. For example, for $\Gamma' = \Gamma$ (while f' remains constant), we would have $[(\Gamma')_s/\Gamma] = 2.9$. (The value of f' enters in a secondary way by affecting $h(t)$; for the case given here, $h(t)$ equals 1.23.)

Nagle et al.²⁷ reported $\Gamma_e/\Gamma = 7.5$ for a Pt source and a 200 mg/cm² (4.1-mil) Au absorber. Since their absorber had an $h(t)$ value of about 1.1, $(\Gamma')_s + \Gamma'$ is equal to 6.8 Γ . If $(\Gamma')_s$ were assumed equal to Γ' , one would obtain $\Gamma' = 3.4$. (Note that the large line width would not have been affected

significantly by the chemical shift of 1.07Γ which we found for a Pt source and an Au absorber.)

Inasmuch as we were not concentrating on line widths, we did not vary nor control the mechanical or heat histories of the solids as one should if line-broadening effects are to be studied systematically. Such studies are to be encouraged because they would give useful information both about variations of local environments in solids and about how $(\Gamma')_s$ and Γ' could be controlled and minimized in order to simplify the interpretation of future Mössbauer experiments.

C. Resonant Absorption and Recoil-Free Fractions

1. Source Calibration

The recoil-free fraction, f , of gamma rays emitted by any source can be found from Eq. (20) or Eq. (21) if a source is calibrated so that t , Γ' , and f' are known. For very precise work, it would be particularly desirable to obtain unambiguous values both of Γ' (such as $\Gamma' = \Gamma$) and of f' (such as might be obtained from independent recoil-free Rayleigh-scattering data¹³). We used a simpler absorber-calibration technique based on the planned similarity of the sources and absorbers on line 1 of Table I. We shall examine below the type of precision that can be obtained with this type of calibration; auxiliary data obtained with the same absorber but with different sources also can help define and limit the absorber parameters.

Three separate sources were prepared by bombarding 10-mil Au foil with 10.75-Mev protons at the Berkeley 60-in. cyclotron. The data summarized on line 1 of Table I is the average of three measurements which agreed well with each other within the statistical accuracy obtained. The composite data are shown together with a Lorentz fit in Fig. 3. The parameters

used for this fit were a peak absorption, $P_{\text{exp}} = 2.4\%$, and a full width at half maximum of 0.62 cm/sec corresponding to $(\Gamma_e/\Gamma) = 6.7$. The implied area is 0.0234 cm/sec . Conservative errors of $P_{\text{exp}} = 0.024 \pm 0.004$ and $\Delta v = 0.62 \pm 0.07 \text{ cm/sec}$ were assigned to try to include systematic errors such as possible deviations of the data from a Lorentz curve.

The inferred results depend on the source and absorber being sufficiently similar so that $(\Gamma')_s = \Gamma'$ and $f = f'$. These assumptions seemed plausible because the three sources gave essentially the same data despite significant differences in proton beam intensities and bombardment times used. (The additional reassurance one might find in the recurrence of the same $(\Gamma')_s$ in many other sources is probably negated by the disquieting unexplained variation of $(\Gamma')_s$ in still other sources, as mentioned above.)

The assumption that $(\Gamma')_s = \Gamma'$ implies that $\Gamma_a = \Gamma_e$ and that Eq. (12) can be used to give Γ' as a function of Γ_e and t . Because of the finite source thickness, the effective $h(t)$ was not that given by Eq. (13). Fortunately, $h(t)$ could be obtained simply from the numerical calculations of Margulies and Ehrmann.¹¹ The distribution of Hg^{197} in the Au source foil, as calculated from the published $\text{Au}^{197} (p, n) \text{Hg}^{197}$ cross section,²⁸ corresponded closely to half of a gaussian curve. The maximum activity was at the foil surface, and it dropped to $1/e$ of this value at a gold thickness of $T_s = 2 \text{ mils}$. For the small values of t , and $T_s/T_A = 0.2$, with which we had to deal, the inclusion of source thickness changed the source broadening function to

$$[h(t)]_{S+A} = 1 + 0.135t [1 + (T_s/T_A)] . \quad (23)$$

For the best value we obtained for t ,

$$[h(t)]_{S+A} = 1.20 \text{ whereas } h(t) = 1.17.$$

Combining the experimental data, the assumptions $(\Gamma')_s = \Gamma'$ and $f = f'$, and Eqs. (12), (16), (17b), (21a), and (23), we obtain

$$0.024 = f p(t) , \quad (24a)$$

$$t = 60.6 f(\Gamma/\Gamma') , \quad (24b)$$

and

$$(\Gamma'/\Gamma) = 3.35 / (1 + 0.162t) , \quad (24c)$$

where $60.6 = n \sigma_m$ for the 10-mil foil, $3.35 = (\Gamma_e/2\Gamma)$, and $0.024 = P_{exp}$.

The derived values of f , $p(t)$, Γ'/Γ , and t are given on the first line of Table II. The errors quoted allow for the extremes of the conservative experimental errors given above. The entries on line 2 of Table II indicate how much error would remain if Γ_a were known precisely.

Derived quantities for Au absorbers, as obtained from the data of Nagle et al.,²⁷ are shown on line 3; these quantities have been adjusted to a foil thickness of 10 mils to simplify direct comparison with other entries in Table II. The values given on line 3 of Table II come from data which were used in an attempt to determine $p(t)$ and hence t by studying the variation of $p(t)$ for different absorber thickness. (Peak absorptions of $4.0 \pm 0.6\%$, $7.7 \pm 0.5\%$, and $11.5 \pm 0.7\%$ were obtained with foils of 100 mg/cm^2 , 200 mg/cm^2 , and 400 mg/cm^2 .) In this procedure it is assumed that Γ' and f' remained the same for all three absorbers. The large error associated with t despite the relatively precise determinations of the peak absorptions reflects the inherent insensitivity of the method; no allowance has been made in the errors for possible variations of Γ' or f' between different absorbers.

In order to obtain f' (for line 3, Table II), it was necessary to estimate Γ' . In the absence of any other relevant data, we could only assume $\Gamma' = (\Gamma')_s$ which implies $\Gamma' = 3.4\Gamma$; there does not seem to be any reasonable way to assign an error to this estimate. If Γ'/Γ is assumed to be exactly 3.4, the originally quoted value²⁷ of 0.03 is multiplied by this factor. (The entry in Table II is 10% higher than this because of the new, larger value of the internal-conversion coefficient.) The error assigned to f' on line 3 does not include any allowance for an error in Γ' .

It is worth emphasizing that the values and errors quoted on lines 1 and 2 of Table II are based solely on the data obtained with the Hg^{197} in Au source and the 10-mil absorber. The additional data and analysis which follows will place further reasonable restrictions on the actual absorber parameters.

2. The Determination of Recoil-Free Emission Fractions

Once an absorber has been calibrated, the recoil-free emission fractions can be calculated directly from the observed absorption with the aid of Eqs. (20). For the 10-mil Au absorber parameters given in Table II, the area is

$$\text{Area} = \pi \left(\frac{0.605 \text{ cm/sec}}{2} \right) (0.413) f$$

or

$$f = \frac{\text{Area under absorption curve}}{0.39 \text{ cm/sec}} \quad (25)$$

If the data in Table II were all that were available, the error in an absolute f value should include, in addition to the error in the area, a 13% error arising in the factor 0.39 because of the extreme acceptable limits of line width and peak absorption. However, if one accepts as a reasonable upper limit on f the Debye model value, f_D , discussed below, the data on line 3 of Table I place a lower limit of about 0.38 cm/sec on the denominator in Eq. (25). An upper limit on this denominator can be obtained by assuming the theoretical upper limit $f' = 0.18$ for the Au absorber, and the maximum value Γ'/Γ consistent with Γ_e and $h(t)$. This gives 0.74 cm/sec in place of 0.39 cm/sec for the denominator in Eq. (25). Thus, without any of the information obtained from the Hg^{197} in Au¹⁹⁷ source, the denominator in Eq. (25) could be rewritten as 0.56 ± 0.18 cm/sec. We shall use Eq. (25) in the following analysis; the f values we derive can be multiplied by 0.70 and an error of 3% can be added to get the alternate f values implied by a denominator of 0.56 cm/sec.

If the Doppler curve is a Lorentzian which has a full width at half maximum of Γ_e or Δv , the f value [equivalent to that in Eq. (25)] can be obtained from Eq. (21a) as:

$$f = \left(\frac{\Delta v}{0.605} \right) \left(\frac{P_{\text{exp}}}{0.413} \right) = \left(\frac{\Gamma_e}{2.78\Gamma} \right) \left(\frac{P_{\text{exp}}}{0.413} \right). \quad (26)$$

Even though the 5-mil Au absorber was not properly calibrated, it is instructive to examine the corresponding equations for f if f' is held constant at 0.058 and Γ' is allowed to vary. For $\Gamma' = 2.78\Gamma$ we have

$$f = \frac{\text{Area under absorption curve}}{0.226 \text{ cm/sec}} \quad (27a)$$

On the other hand for $\Gamma' = \Gamma$ we have

$$f = \frac{\text{Area under absorption curve}}{0.19 \text{ cm/sec.}} \quad (27b)$$

The near equality of Eqs. (27a) and (27b) emphasizes that f can be determined rather accurately despite a lack of knowledge of Γ' , provided f' is known. Note that whereas Eq. (21a) corresponds to $t = 0.63$, Eq. (21b) corresponds to $t = 1.73$; this is merely an illustration of the utility of Eq. (20b) which shows that f is more sensitive to f' than to t .

In the more standard case, when a calibrated absorber is used to determine the f value of different sources, f' and Γ' must be known for the source in addition to t . (Of course if t is known, either f' or Γ' implies the other from Eqs. (8) and (17b).) For example, consider the data reported by the Los Alamos group²⁷ for a 200 mg/cm² Au absorber with $t = 0.83$, which gave 7.7% peak absorption with a Pt source. For this example Eq. (21b) gives

$$0.077 = 25 \frac{1}{7.5} ff' [0.83]$$

or

$$ff' = 0.028. \quad (28)$$

Neither f' nor f can be found unless some auxiliary condition is used. One possibility would be to use $t = 25f' \Gamma/\Gamma'$. Then for $\Gamma'/\Gamma = 3.4$, as suggested above, we would have $f' = 0.11$ and $f = 0.25$. However, other Γ'/Γ values would give other combinations. Fortunately, theoretical predictions of the Debye model make it seem likely that we would have $f' \leq 0.18$ and $f \leq 0.30$. With these restrictions, the extreme values implied by Eq. (28) are $f' = 0.18$, $\Gamma'/\Gamma = 1.8$, and $f = 0.15$, or $f = 0.30$, $f' = 0.043$, and $\Gamma'/\Gamma = 3.5$. Of course, these extremes would be increased if errors in the 7.7% peak absorption and in the 0.83 value used for t were taken into account.

3. Observed Recoil-Free Emission Fractions

The observed absorption areas are listed in column VI of Table I. These values have been corrected for background including radiations other than the 77-kev gamma rays. The areas also include a correction of about 15% because there was some resonant absorption even at the highest velocities used. (This correction was made by assuming that the Lorentz line which fitted the data near the peak absorption continued to be valid at relatively high velocities.) We have attempted to include in the assigned errors uncertainties both in these corrections and in the decay corrections that were made. The values of $100f$ listed in column VII were derived from Eq. (25) (for lines 3 through 8); the errors are those due to area uncertainty only. As mentioned above, the uncertainty in Eq. (25) would contribute an additional 13% to the absolute f values, but it would not change the relative f values.

The f value appearing on line 2 of Table I is based on Eqs. (27a) and (27b), and includes the error implied by the inequality of these equations. However, no allowance is made for a possible difference in f' between the 5-mil and 10-mil Au absorbers. The f value given for the Hg^{197} source of line 1 was determined as part of the source calibration described above.

It is customary to compare observed f values with those predicted by the Debye model of a solid. If the Au nucleus were free to recoil it would have an energy $(P^2/2M) = 0.016$ ev; this energy divided by Boltzmann's constant gives a temperature, $\bar{\Phi}$, of 185°K . According to the Debye model, for very low temperature, f should be given by the temperature-independent Debye-Waller factor^{1, 9, 29, 30, 31}

$$f_D = \exp(-3\bar{\Phi}/2\theta_D), \quad (29)$$

where θ_D is the Debye temperature.

Column VIII gives the f_D values calculated from Eq. (29) by using the Debye temperatures listed in Column IX.^{32, 33} One can also define an effective Mössbauer crystal temperature θ_{eff} [based on Eq. (29)] by

$$\theta_{\text{eff}} = 3\bar{\Phi}/2 \ln\left(\frac{1}{f}\right) = 278^\circ\text{K} / \ln\left(\frac{1}{f}\right). \quad (30)$$

The θ_{eff} values obtained from Eq. (30) are given in Column X of Table I.

Most of the f values in Table I are lower than the f_D values; correspondingly θ_{eff} is less than θ_D . It is not surprising that the simple Debye model fails; other failures have been noted.^{27, 30, 34} However, these small f values do not necessarily imply that the Debye model is totally inadequate for predicting f and its temperature dependence.^{1, 9, 30} For example, the Debye model might explain accurately the behavior of a fraction f/f_D of the source atoms which might be tightly bound to the lattice while the remaining $1-(f/f_D)$ atoms might not have proper lattice sites. On the other hand, all of the radioactive source atoms might be in similar sites, and the Debye-model predictions might be obeyed if θ_{eff} were substituted for θ_D . It therefore seems best to reserve judgment about the implication of these small f values until f is measured as a function of temperature.³⁴

Because the most likely mechanisms that explain the inequality of f and f_D imply $f \leq f_D$, the high f value obtained with the Pt^{197} in Pt source (line 3) can be used to set a reasonable lower limit on the factor in Eq. (20a), $\pi c \Gamma' h(t) p(t) / E_0$, for the 10-mil absorber. This lower limit is 0.38 cm/sec, which is quite close to the value used in the denominator of Eq. (25). Thus, the f values given on lines 1 and 3 to 8 of Table I are close to the maximum values consistent with the 10-mil absorber. (That is, the uncertainty in Eq. (25) no longer can raise the f values by more than 3%, although this uncertainty could still reduce the values by 13%.) The upper extreme value of $\pi c \Gamma' h(t) p(t) / E_0$ for the 10-mil absorber is limited by the conditions $f' \leq f_D = 0.18$ and, from line 4, $5 \Gamma \geq (\Gamma' + \Gamma) h(t)$, where $t = 60.6 f' \Gamma / \Gamma'$. These conditions give a maximum of 0.74 cm/sec for the denominator of Eq. (25), which implies only that the f values in Table I could be reduced to as little as 53% of the listed values if the assumptions used in Eq. (25) were wrong.

The high f values obtained with Pt^{197} alloyed with iron, cobalt, and nickel points encouragingly to the enhancement of recoil-free fractions by the proper choice of host. A naive, qualitative description of the important parameters can be given. The importance of a high Debye temperature to large f values [as shown in Eq. (29)] was emphasized when the Mössbauer effect was discovered.¹ When impurity atoms are put into a host lattice, it seems reasonable that they must be bound strongly to their local sites to give large recoil-free effects.³¹ If a recoil-free effect is considered as the correlated recoil of a large number of atoms, the local binding is an indication of the degree to which the impurity atom moves its nearest neighbors, while the properties of the host material govern the number of host atoms which share the recoil momentum. The strength of

the local binding does not depend solely on the Debye temperature of the host.³¹ As has been emphasized,³¹ some Debye temperatures are high because of the low mass of the host atoms rather than large interatomic forces. However, the interatomic forces in a pure host crystal do not necessarily govern the local binding; strong chemical and size effects may exist. Furthermore, even if strong local binding has been achieved, a high Debye temperature of the host would continue to be important. It seems clear that considerable additional experimental and theoretical studies will be needed before f values can be predicted for impurity atoms.

The f values of the sources produced in situ also deserve further attention. The Pt^{197} in Pt sources (lines 2 and 3) had f values close to f_D , in agreement with the results of recoil-free Rayleigh scattering by Pt.¹³ In contrast, both the Hg^{197} -in-Au and the Hg^{197} -in-Pt sources gave f values significantly lower than f_D . In all four cases, the metal hosts almost surely readjusted to the Au^{197} before the 77-kev photon was emitted. One obvious difference between these two cases is that the high f values occurred when the radioactive nuclei received relatively low recoil energies accompanying neutron capture (i. e., of the order of 10 ev), whereas the low f values were found in sources in which the reacting nuclei recoiled violently (with about 50 kev of energy or more) because of the incident charged particle.

This correlation suggests that radiation damage might be responsible for the low f values. (If this were true the assumption $f' = f$ used to calibrate the source would be unwarranted, and the alternate limits on the f values mentioned above would be more appropriate. Even if f did not equal f' in this case, the identical source and absorber technique has great potentiality.) On the other hand, these data by no means establish the role of radiation damage in producing low f values. For example, if radiation damage did influence the

environment of the radioactive nuclei, one might expect line broadening; thus the particularly narrow line observed with the Hg^{197} in Pt sources would be particularly hard to understand. Furthermore, standard radiation damage studies indicate that most of the radiation damage anneals rather quickly at room temperature.³⁵ More experimental studies will be needed to determine whether the severe local damage accompanying charged-particle absorption persists and is responsible for the low f values.

D. Chemical Shifts

The possibility of a gamma-ray energy shift because of different chemical environment seemed to be recognized in earlier Mössbauer experiments,^{36, 37} but the first precise report of a chemical shift was made by Kistner and Sunyar, who succinctly summarized some of its important implications.³⁸ Since then, other chemical shifts have been observed,^{39, 40} and some have been analyzed in detail.^{41, 42} The shifts we have observed are noteworthy partly because they are so large and partly because one might expect a relatively direct analysis to yield new information about nuclei and solids.

A chemical shift is produced in a Mössbauer experiment by the same coulomb-interaction energy that produces an isotope shift in optical spectra.⁴³ The optical isotope shift occurs when an optical electron experiences a different coulomb-interaction energy with the nucleus depending on the atomic state of the electron; the shift derives its name from the different coulomb potentials produced at the electron by two different isotopes of the same element. An isomer shift has also been observed;⁴⁴ in this case, the energy of an optical transition is affected by the different coulomb interactions caused by two different isomeric states of the same nucleus.⁴⁵ The same interaction energy that produces the isomer shift produces the Mössbauer chemical shift.

However, in this latter case, instead of an optical photon, the nuclear gamma ray is shifted in energy if the nuclear states have different radial charge distributions and if the electron density at the nucleus is different in the source from that in the absorber. (Note that the term "chemical" descriptively implies that the shift is to be expected if the electron density at the origin is changed, as it would be in different chemical environments.)

The observed chemical shifts are given in Column XI of Table I in units of the natural line width, $\Gamma = 2.4 \times 10^{-7}$ ev. Typical Doppler curves which show these shifts for different parents in Pt are given in Fig. 4. Note that the shift for Hg^{197} in Pt is essentially the same as the shift for Pt^{197} in Pt; thus the shift does not seem to be particularly correlated with either f or Γ_e . The chemical shifts for stainless steel is shown in Fig. 5 while the shifts for Fe, Co, and Ni are given in Fig. 6. For the Fe and Co hosts the quoted shift is the center of area (which is also the midpoint between the two hyperfine peaks).

All of the energy shifts reported in Table I involve emitted gamma rays whose energy is greater than that required for resonance at the absorber. The presence of electron charge density at the nucleus tends to decrease the energy of each of the nuclear states. The total energy of the system would be lowest if the positive nuclear charge were concentrated at the center (i. e., at $r = 0$.) If the excited nuclear state has a smaller charge radius, a larger electron density will decrease its energy relative to the ground state, thereby reducing the nuclear transition energy. Thus, if the excited nuclear state has a smaller effective charge radius (as implied by the nuclear shell model), the electron density at Au nuclei is higher in a Au lattice than it is in the other host materials we have investigated.

It is instructive to make an order-of-magnitude estimate of the expected chemical shift. Consider only the charge density contributed at the nucleus by the outermost (6s) electron in Au. For a free Au atom the charge density at the nucleus due to a nonrelativistic electron would be about 2.2×10^{13} coul/m³ corresponding to a potential $V = -V_0 + 4.2 \times 10^{-7} r^2$ volts, where r is the radial distance in fermis. Since a proton at the edge of the potential well of a Au nucleus has a value of $r^2 = 42$ (fermis)², moving a proton from the origin to the edge of the well raises the energy of the state by 18×10^{-6} ev because of the presence of the 6s electron alone.

The expected shift in this approximation can be obtained by using a nuclear model to find the average value $\langle r^2 \rangle$. First consider only the outermost proton whose radial distance will be denoted by the subscript 0. If the ground state of Au¹⁹⁷ is identified as a $d_{3/2}$ single-particle state, the proton is in a 2d orbit.⁴⁶ Similarly, the excited state corresponds to a 3s proton orbit if the $s_{1/2}$ assignment is valid. If harmonic-oscillator wave functions are used, we have $\langle r_0^2 \rangle_{2d} = \langle r_0^2 \rangle_{3s}$ inasmuch as the 2d and 3s states are degenerate in the harmonic-oscillator model. (Thus, harmonic oscillator wave functions are not adequate to describe this nucleus insofar as chemical shifts are concerned.) On the other hand, the finite square-well model gives⁴⁷ $\langle r_0^2 \rangle_{2d} \simeq 0.47 R_v^2$ and $\langle r_0^2 \rangle_{3s} \simeq 0.41 R_v^2$. This implies that the nuclear transition energy would increase by about 1.1×10^{-6} ev if the (nonrelativistic) 6s electron were removed from the atom. This is certainly the correct order of magnitude inasmuch as the largest shifts in Table I are about $5\Gamma = 1.2 \times 10^{-6}$ ev. Relativistic effects will increase the estimated shift because they increase the electron density at the origin. More exact calculations of the expected chemical shift are being made by one of us (D. A. S.).

Unfortunately, the energy shift may be seriously affected by changes in the entire charge radius. To estimate this effect, consider the change,

$\Delta \langle r^2 \rangle$, expected for a change from A to $A + 1$ (as might be found in a standard isotope shift.). In this case, we have $(\Delta \langle r^2 \rangle) / \langle r^2 \rangle = 1/300$ or $\Delta \langle r^2 \rangle = R_v^2/600$. However, because 79 protons would be affected, this is equivalent to a change in a single proton $\Delta \langle r_0^2 \rangle$ of about $(79/600) R_v^2$ or $0.13 R_v^2$. Typically,^{43, 48} observed isotope shifts are about one-half of the expected shifts, implying that an experimental isotope shift might give about the same $\Delta \langle r_0^2 \rangle$ as the finite square-well model predicts for a $3s \rightarrow 2d$ proton transition. Inasmuch as the isomer shift produced about 20 to 25% of the isotope shifts seen in Hg, and inasmuch as the two isomeric neutron states in Hg are very different ($p_{1/2}$ and $i_{13/2}$ corresponding to $3p$ and $1i$ which have $\Delta \langle r_0^2 \rangle$ differing by about $R_v^2/4$), the $\Delta \langle r_0^2 \rangle$ expected from $Z\Delta \langle r^2 \rangle$ is probably considerably smaller than $\Delta \langle r_0^2 \rangle$ from the proton for Au^{197} . (This conclusion should be considered as a reasonable working hypothesis rather than an established fact, because too little is known about isomer shifts. For example, contradictory conclusions⁴² seem to come from the effective $\Delta \langle r_0^2 \rangle$ found from the chemical shift caused by a neutron transition in Fe^{57} .)

Despite the uncertainties that exist at present, there is little doubt about the ultimate importance of chemical shift data, particularly with odd-proton nuclei. From a solid-state viewpoint, the data now can give relative electron densities at nuclei of impurities. (For example, the data in Table I show clearly that the electron density at Au nuclei is greatest when Au is the host, almost as great in a Pt host, significantly smaller in a Ni host, and smallest in an Fe host.) Future theoretical and experimental advances should make it possible to obtain absolute electron-density data.

The ratio of the electron density at the nucleus in a metal to the density in a free atom is a key parameter in the Knight shift of a nuclear-magnetic-resonance line due to chemical effects.⁵⁰ The Mössbauer chemical shift can give this parameter more directly, and can check the degree to which this parameter depends solely on the host material when impurity Mössbauer atoms are used.⁵⁰ From a nuclear-physics point of view, chemical-shift data should add significantly to and perhaps help clarify evidence about nuclear charge distribution available from optical-isotope and isomer shifts.

E. Nuclear Zeeman Splitting and Local Magnetic Fields

The precise energy resolution inherent in Mössbauer absorption makes it possible to observe Zeeman splitting of nuclear gamma rays.^{51, 52} (If the responsible magnetic field is produced by atomic electrons, the splitting is analogous to atomic hyperfine structure.) The magnetic splitting of the 14-keV Fe⁵⁷ line was observed independently by several groups,⁵³⁻⁵⁶ and a detailed analysis was given which led to a determination of the local magnetic field at the Fe⁵⁷ nucleus in Fe of -3.3×10^5 oersteds.⁵⁶ Local magnetic fields have also been reported at Fe⁵⁷ nuclei in a variety of host materials.^{37, 38, 57-60} Magnetic splitting and local fields in some hosts have also been reported for the Sn¹¹⁹ Mössbauer transition.^{39, 40} Indications of magnetic effects have also been observed with⁶¹ Dy¹⁶¹ and with⁶² Ni⁶¹.

The only two cases in which we observed magnetic splitting were for Fe and Co hosts as shown in Fig. 6. The energy difference between the two lines in Fe was $(11.9 \pm 0.4)\Gamma$ (or 1.11 cm/sec or 2.86×10^{-6} ev or 0.024 cm^{-1} .) For the Co host the splitting was $(5.2 \pm 0.4)\Gamma$, and for Ni it was $\leq \Gamma$. The expected Zeeman energy levels for the single-particle-model states are shown in Fig. 7. If the magnetic field were not strong enough to separate the ground-state Zeeman levels significantly, the expected pattern would consist of two

equal-intensity lines separated by an energy corresponding to the magnetic splitting of the excited state.

Since the magnetic moment of the excited state is unknown, the local magnetic field cannot be given. (An experiment is being done with a strong known external magnetic field in order to determine the magnetic moment of the excited state and to find the direction of the local magnetic field. This experiment will be analogous to those performed with Fe⁵⁷ and with Sn¹¹⁹.⁴⁰) However, the expected shell-model value of 1.6 nm mentioned in Section III above can be used to estimate the magnetic field. The implied local magnetic fields are compared to other related local field determinations in Table III. The large differences we find seem to be similar to those that were found when Sn was in these same host materials.⁴⁰

Our results for Au in Fe are inconsistent with the very high value of the local field reported from low-temperature nuclear-polarization experiments.⁶³ Although our value for the local magnetic field may change somewhat if the excited-state magnetic moment differs from 1.6 nm, it is very doubtful that the local field can be very much higher than the 282×10^3 oe listed. If the field were greater than 10^6 oe as suggested,⁶³ the Zeeman levels of the nuclear ground state of Au would be split enough to produce unmistakable broadening of the Doppler pattern beyond that shown in Fig. 6. The reported 10^6 oe for Au in Fe could be reduced to agree with the value we obtain if one postulates that the actual low temperature attained in the polarization experiment was about one-third of the reported value, which seems unlikely. In view of the assumptions made in both types of experiment, a conclusive discussion of this point must be deferred until more data are available. At this point we can say only that a serious discrepancy apparently exists.

The third line that appears in the Fe Doppler pattern at about +0.7 cm/sec (i. e., shifted by 7.5Γ) is probably not part of the Zeeman pattern. The intensity of this line varied unpredictably in the three Au in Fe samples we used, even though the positions of the two other Zeeman lines were accurately reproducible (to within one-half the quoted limits of error.) Therefore this third line seems to imply that there are Fe lattice sites at which the Au nuclei do not experience a strong local field.

ACKNOWLEDGMENTS

We wish to thank F. Asaro and H. Robinson for making available the proportional counter used in our experiments, and J. G. Conway for the use of his furnace in preparing alloys. We also appreciate helpful discussions with A. M. Portis and L. D. Roberts.

One of us (P. A.) would like to thank Professors I. Perlman and J. O. Rasmussen for the kind hospitality extended to him while he was a summer visitor. He would also like to thank his colleagues at Illinois for illuminating discussions; particularly valuable help was obtained from D. G. Ravenhall, J. D. Jackson, H. Frauenfelder, E. Lüscher, S. Margulies, J. S. Koehler, and F. Seitz.

Table I. Summary of experimental data for recoil-free resonant absorption of the 77-kev γ -ray of Au^{197} in several metals

I	II	III	IV	V	VI	VII	VIII	IX	X	XI	
Parent	Production reaction	Host	Au absorber thickness (Mils)	$\frac{\Gamma_e}{\Gamma}$ ^a	Absorption area (0.01 cm/sec)	100f	100f _D	θ_D	θ_{eff}	Chemical shift $\Delta E/\Gamma$ ^{a, b}	
<u>Group A</u>											
1	Hg^{197}	$\text{Au}^{197}(\text{p}, \text{n})$	Au	10	6.7 ± 0.8	2.34 ± 0.70	5.8 ± 0.9	18	185	98	0 ± 0.54
2	Pt^{197}	$\text{Pt}(\text{n}, \gamma)$	Pt	5	4.4 ± 0.2	6.0 ± 0.4	29 ± 5	30	233	218	--
3	Pt^{197}	$\text{Pt}(\text{n}, \gamma)$	Pt	10	6.6 ± 0.3	13.4 ± 3.0	34 ± 8	30	233	248	1.07 ± 0.21
4	Hg^{197}	$\text{Pt}(\alpha, 3\text{n})$	Pt	10	4.8 ± 0.2	5.6 ± 0.4	14.3 ± 1.1	30	233	137	--
<u>Group B</u>											
5	Pt^{197}	$\text{Pt}^{196}(\text{n}, \gamma)$	S. S. ^c	10	8.0^{d}	8.9 ± 3.0	24 ± 9	--	--	--	5.53 ± 0.54
6	Pt^{197}	$\text{Pt}^{196}(\text{n}, \gamma)$	Fe	10	$6.5 \pm 1.0^{\text{e}}$	12.4 ± 3.0	32 ± 8	55	467	243	5.91 ± 0.37
7	Pt^{197}	$\text{Pt}^{196}(\text{n}, \gamma)$	Co	10	$7.0 \pm 0.8^{\text{e}}$	10.5 ± 2.5	27 ± 7	53	445	205	5.12 ± 0.33
8	Pt^{197}	$\text{Pt}^{196}(\text{n}, \gamma)$	Ni	10	6.5 ± 0.6	13.8 ± 2.5	35 ± 7	53	441	255	4.62 ± 0.33

^a Γ is the natural width which equals 2.4×10^{-7} ev or 9.3×10^{-2} cm/sec.

^bAll shifts correspond to emitted gamma ray whose energy is too high for resonant absorption.

^cS. S. indicates stainless steel.

^dNon-Lorentzian; quoted value is full width at half maximum.

^eEstimate of each component of line with structure.

Table II. Derived parameters of the resonance line obtained with a source of Au¹⁹⁷ in gold and a gold absorber

Assumed conditions		Derived quantities			
Peak absorption (%)	Γ_e/Γ	100f'	$\rho(t)$	Γ'/Γ	t
2.4±0.4	6.7±0.8	5.8±0.9	0.41±0.06	2.78 ^{+0.62} _{-0.42}	1.26±0.27
2.4±0.4	6.7±0.0	5.8±0.6	0.41±0.03	2.78±0.06	1.26±0.17
Reference 27 corrected to 10-mil Au		11 ± 4	0.53±0.10	3.4	2.03±0.69

Table III. Local field in kiloersteds^a

Impurity atom	Hosts			Reference
	Fe	Co	Ni	
Au	282±10	122±10	≤ 30	This work
Au	>1000			63
Fe	-330	310	260	37, 64
Co	-320	-220	-80	58, 65-68
Ni			170	58
Sn	-81	- 20	+18	40
In	>250		~0	63
Sb	>280			63
Sc	~100			69

^aThe signs of the local fields are unknown except where given.

REFERENCES

*This work was supported at the University of California by the U. S. Atomic Energy Commission, and at the University of Illinois by the joint program of the U. S. Atomic Energy Commission and the Office of Naval Research.

†Summer visitor to Lawrence Radiation Laboratory, 1960.

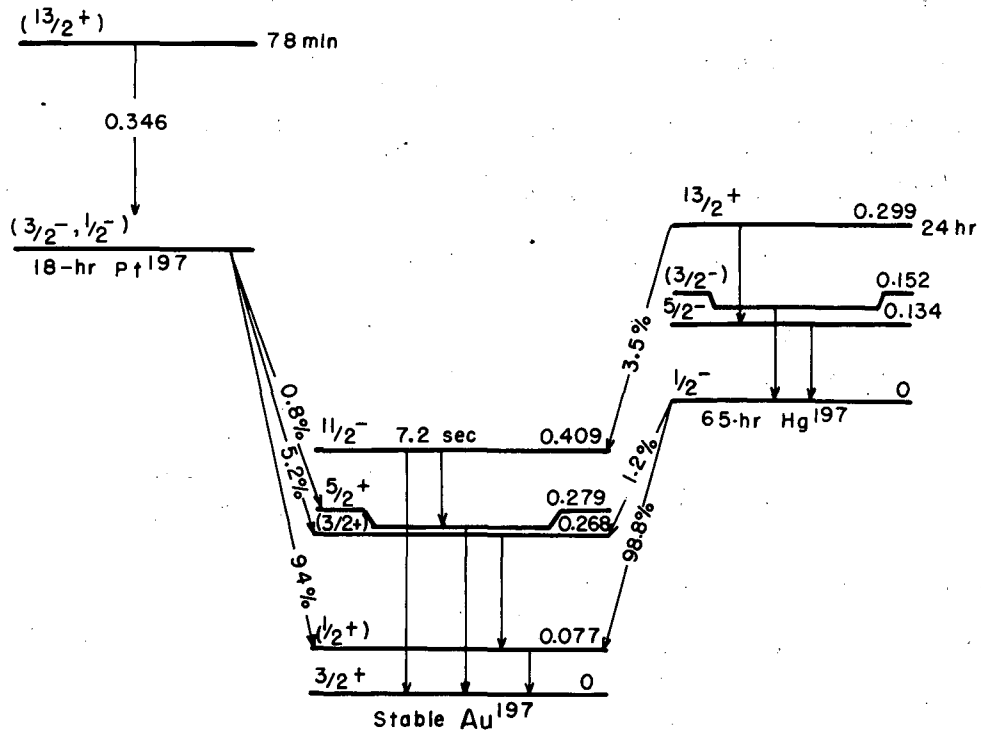
1. R. L. Mössbauer, Z. Physik, 151, 125 (1958); Naturwissenschaften 45, 538 (1958); Z. Naturforsch. 14a, 211 (1959).
2. G. Breit and E. P. Wigner, Phys. Rev. 49, 904 (1936).
3. H. A. Bethe and G. Placzek, Phys. Rev. 51, 450 (1937).
4. H. A. Bethe, Revs. Modern Phys. 9, 69 (1937).
5. W. W. Havens, Jr. and J. Rainwater, Phys. Rev. 83, 1123 (1951); Phys. Rev. 92, 702 (1953); this paper also contains references to earlier papers which included relevant graphs.
6. G. V. Dardel and R. Persson, Nature 170, 1117 (1952).
7. See, for example, D. J. Hughes, J. Nuclear Energy 1, 237 (1955); or J. Rainwater, Handbuch der Physik, S. Flügge, Ed. (Springer Verlag, Berlin, Germany, 1957), Vol XL. p. 373.
8. W. M. Visscher, (unpublished, privately circulated notes), Los Alamos Scientific Laboratory, Los Alamos, New Mexico.
9. E. Cotton, J. Phys. and Rad. 21, 23 (1960).
10. R. L. Mössbauer and W. H. Wiedemann, Z. Physik 159, 33 (1960).
11. S. Margulies and J. Ehrmann, University of Illinois, Urbana, Illinois, private communication.
12. J. D. Jackson, Can. J. Phys. 33, 575 (1955).
13. C. Tzara and R. Barloutand, Phys. Rev. Letters 4, 405 (1960).

14. K. Way et al., Nuclear Data Sheets, National Academy of Sciences, National Research Council.
15. J. W. Mihelich and A. de-Shalit, Phys. Rev. 91, 78 (1953).
16. R. Joly, J. Brunner, J. Halter, and O. Huber, Helv. Phys. Acta 28, 403 (1955); Helv. Phys. Acta 26, 591 (1953).
17. L. A. Sliv and I. M. Band, Coefficients of Internal Conversion of Gamma Radiation, Academy of Sciences of the U. S. S. R., Part I. K Shell (1956); Part II. L Shell, (1958); (English Translations: University of Illinois Reports 57 ICC K1 and 58 ICC L1, April 1957).
18. M. E. Rose, Internal Conversion Coefficients, (North Holland Publishing Company, Amsterdam, Netherlands, 1958).
19. A. W. Sunyar, Phys. Rev. 93, 653 (1955).
20. S. A. Moszkowski, Phys. Rev. 83, 1071 (1951); V. F. Weisskopf, Phys. Rev. 83, 1073 (1951); M. Goldhaber and J. Weneser. Annual Review of Nuclear Science (Annual Reviews, Inc., Palo Alto, California, 1956), Vol. 5, p. 1.
21. R. M. Elliott and J. Wulff, Phys. Rev. 55, 170 (1939).
22. D. Strominger, J. M. Hollander, and G. T. Seaborg, Revs. Modern Phys. 30, 585 (1958).
23. J. E. Mack, Revs. Modern Phys. 22, 64 (1950).
24. E. M. Bernstein and H. W. Lewis, Phys. Rev. 100, 1345 (1955).
25. F. K. McGowan and P. H. Stelson, Phys. Rev. 109, 901 (1958).
26. K. Alder, A. Bohr, T. Huus, B. Mottelson, and A. Winther, Revs. Modern Phys. 28, 432 (1956).
27. D. Nagle, P. P. Craig, J. G. Dash, and R. R. Reiswig, Phys. Rev. Letters 4, 237 (1960).
28. R. Vandenbosch and J. R. Huizenga, Phys. Rev. 120, 1313 (1960).

29. I. Waller, *Ann. Physik* 79, 261 (1926). See also A. H. Compton and S. K. Allison, *X-rays in Theory and Experiment* (D. Van Nostrand Co., New York 1935), p. 435.
30. W. M. Visscher, *Ann. Phys.* 9, 194 (1960).
31. H. J. Lipkin, *Ann. Phys.* 9, 332 (1960).
32. P. H. Keesom and N. Pearlman, *Handbuch der Physik*, S. Flügge, Ed. (Springer Verlag Berlin 1956), Vol. XIII, p. 282.
33. J. A. Rayne and W. R. G. Kemp, *Phil. Mag.* (8) 1, 918 (1956).
34. A. J. F. Boyle, D. St. P. Bunbury, C. Edwards, and H. E. Hall. *Proc. Phys. Soc. (London)* 76, 165 (1960).
35. F. Seitz and J. S. Koehler, *Solid State Physics Vol 2*, (Academic Press, New York N. Y., 1956) p. 307; see also articles by J. S. Koehler and by Blewitt, Coltman, Holmes, and Noggle in *Dislocations and Mechanical Properties of Crystals* (John Wiley and Sons Co., New York, 1957).
36. R. V. Pound and G. A. Rebka, Jr., *Phys. Rev. Letters* 4, 337 (1960) and R. V. Pound and G. A. Rebka, Jr., *Phys. Rev. Letters* 4, 397 (1960).
37. G. K. Wertheim, *Phys. Rev. Letters* 4, 403 (1960).
38. O. C. Kistner and A. W. Sunyar, *Phys. Rev. Letters* 4, 412 (1960).
39. S. S. Hanna, L. Meyer-Schutzmeister, R. S. Preston, and D. H. Vincent, *Phys. Rev.* 120, 2211 (1960).
40. A. J. F. Boyle, D. St. P. Bunbury, and C. Edwards, *Phys. Rev. Letters* 4, 553 (1960).
41. S. DeBenedetti, G. Lang, and R. Ingalls, *Phys. Rev. Letters* 6, 60, (1961).
42. L. R. Walker, G. K. Wertheim, and V. Jaccarino, *Phys. Rev. Letters*, 6, 98 (1961).

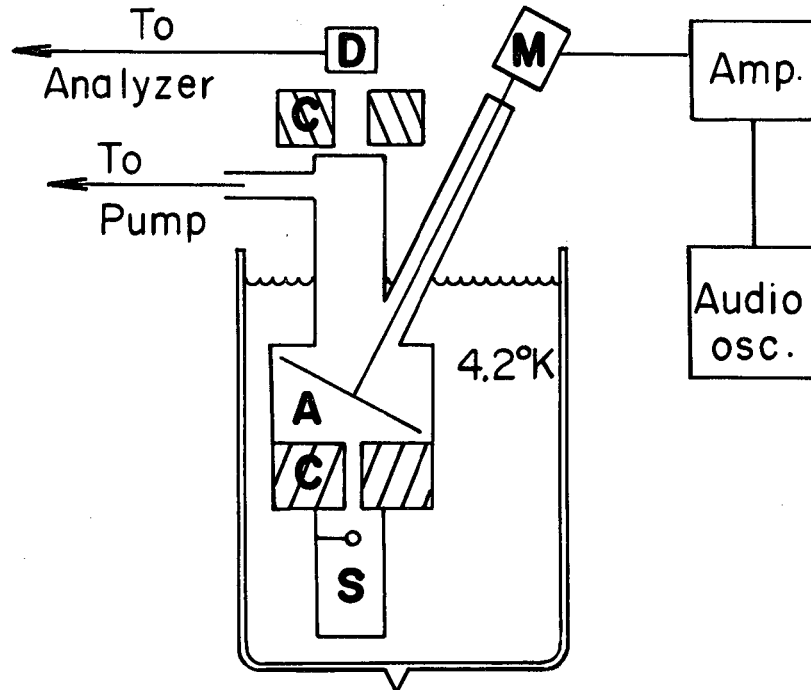
43. For an excellent summary see G. Breit, *Revs. Modern Phys.* 30, 507 (1958).
44. A. C. Melissinos and S. P. Davis, *Phys. Rev.* 115, 130 (1959).
45. R. Weiner, *Phys. Rev.* 114, 256 (1959).
46. See any of the fine reviews of the single-particle shell model such as M. Goeppert Mayer and J. H. D. Jensen, Elementary Theory of Nuclear Shell Structure (Wiley and Sons Co., New York 1955) or E. Feenberg, Shell Theory of the Nucleus (Princeton University Press, Princeton, N. J., 1955).
47. J. Eisinger and V. Jaccarino, *Revs. Modern Phys.* 30, 528 (1958).
48. P. Brix and H. Kopfermann, *Revs. Modern Phys.* 30, 517 (1958).
49. A. C. Melissinos, *Phys. Rev.* 115, 126 (1959).
50. W. D. Knight, Solid State Physics Advances Vol. 2, (Academic Press, New York, 1956).
51. This application undoubtedly occurred to many independently, but the first published mention of it resulted from independent suggestions by M. Hamermesh and R. Mössbauer to the authors of reference 52.
52. L. L. Lee, L. Meyer-Schutzmeister, J. P. Schiffer, and D. Vincent, *Phys. Rev. Letters* 3, 223 (1959).
53. R. V. Pound and G. A. Reika, Jr., *Phys. Rev. Letters* 3, 554 (1959).
54. G. DePasquali, H. Frauenfelder, S. Margulies, and R. N. Peacock, *Phys. Rev. Letters* 4, 71 (1960).
55. G. J. Perlow, S. S. Hanna, M. Hamermesh, C. Littlejohn, D. H. Vincent, R. S. Preston, and J. Heberle, *Phys. Rev. Letters* 4, 74 (1960).
56. S. S. Hanna, J. Heberle, C. Littlejohn, G. J. Perlow, R. S. Preston, and D. H. Vincent, *Phys. Rev. Letters* 4, 177 (1960).

57. G. K. Wertheim, Mössbauer Effect Conference, University of Illinois Report TN 60-698 AD (1960), unpublished.
58. G. K. Wertheim, Bull. Am. Phys. Soc. II 5, 428 (1960).
59. G. K. Wertheim, Mössbauer Effect in Magnetic Materials, invited paper, Am. Phys. Soc. Thanksgiving Meeting, November 26, 1960).
60. D. E. Nagle, H. Frauenfelder, R. D. Taylor, D. R. F. Cochran, and B. T. Matthias, Phys. Rev. Letters 5, 364 (1960).
61. S. Ofer, P. Avivi, R. Bauminger, A. Marinov, and S. G. Cohen, Phys. Rev. 120, 406 (1960).
62. F. E. Obenshain and H. H. F. Wegener, Phys. Rev. (in press).
63. B. N. Samoilov, V. V. Sklyarevskii, and E. P. Stepanov, Soviet Phys. -JETP 11, 261 (1960).
64. S. S. Hanna, J. Heberle, G. J. Perlow, R. S. Preston, and D. H. Vincent, Phys. Rev. Letters 4, 513 (1960).
65. Y. Koi, to be published in J. Phys. Soc. (Japan) (private communication to the authors from A. M. Portis, Dept. of Physics, University of California, Berkeley, February, 1960).
66. J. G. Dash, R. D. Taylor, P. P. Craig, D. E. Nagle, D. R. F. Cochran, and W. E. Keller, Phys. Rev. Letters 5, 152 (1960).
67. V. Arp, D. Edmonds, and R. Petersen, Phys. Rev. Letters 3, 212 (1959).
68. A. C. Gossard and A. M. Portis, Phys. Rev. Letters 3, 164 (1959); also private communication to the authors from A. M. Portis, Dept. of Physics, University of California, Berkeley, February, 1960.
69. A. V. Kogan, V. D. Kul'kov, L. P. Nikitin, N. M. Reinov, I. A. Sokolov, and M. F. Stel'makh, Soviet Phys. J. E. T. P. (U. S. S. R.) 39, 47 (1960).



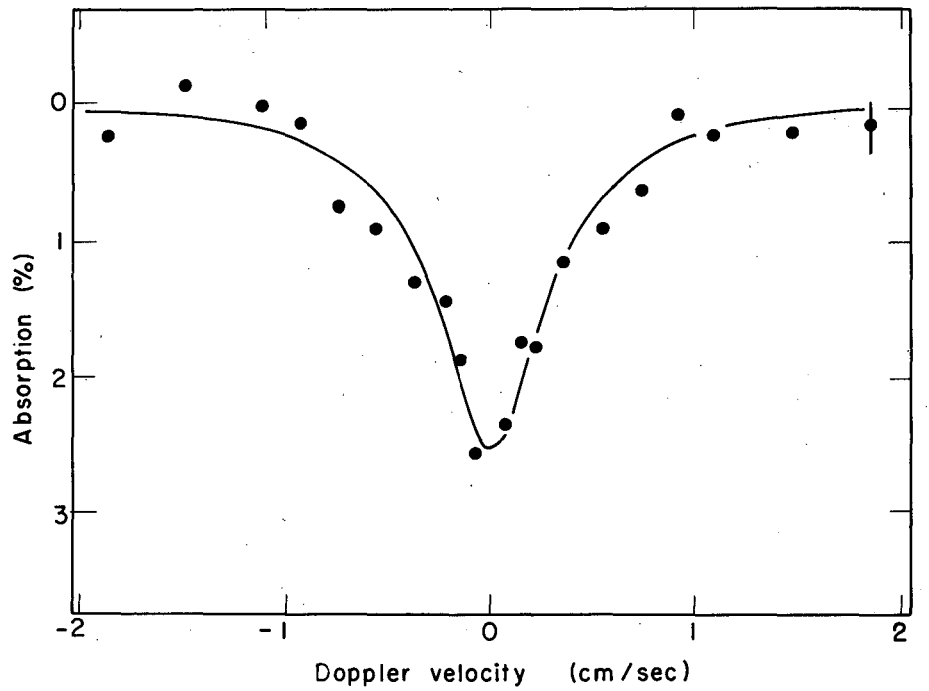
MU - 22651

Fig. 1. Energy levels of Au^{197} populated in the decay of Pt^{197} and Hg^{197} (see reference 14).



MU - 21541

Fig. 2. Schematic diagram of experimental apparatus.
The various components are described in the text.



MU-22650

Fig. 3. Velocity-absorption spectrum of 77-keV γ -ray from Au^{197} in gold. The data have been corrected for the contribution from 66-keV Au x-rays. The statistical uncertainty is indicated on one point. The curve drawn is the best Lorentz fit to the data.

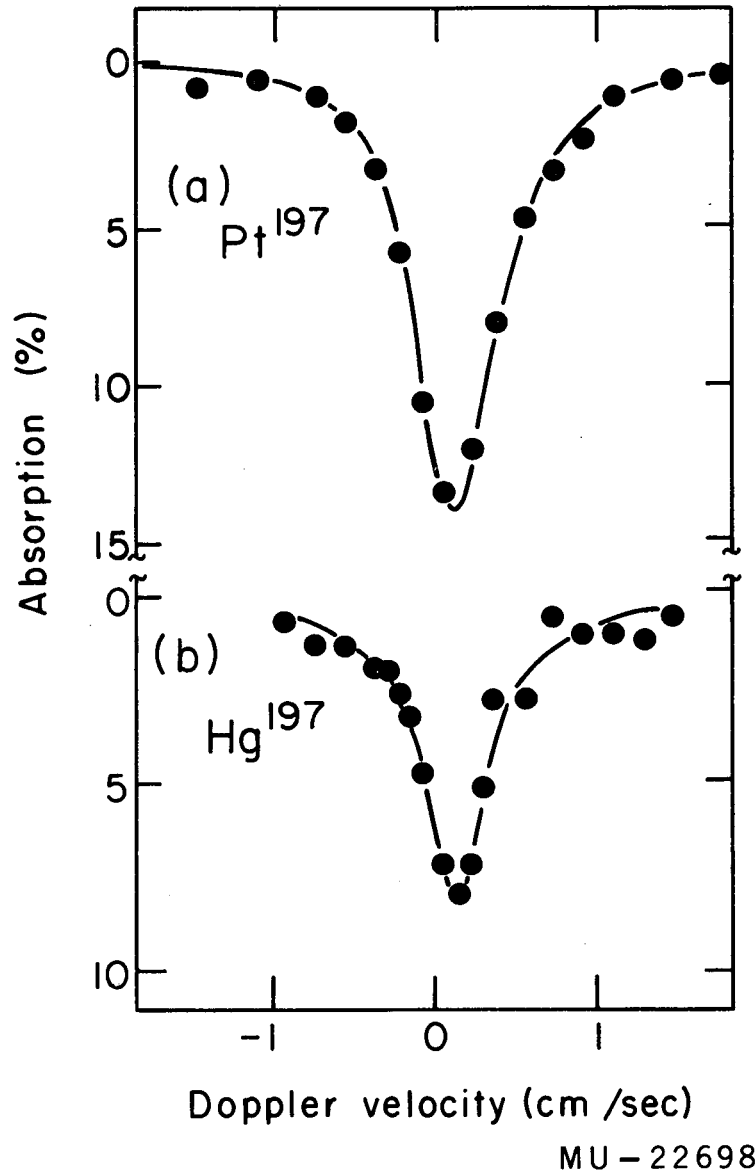
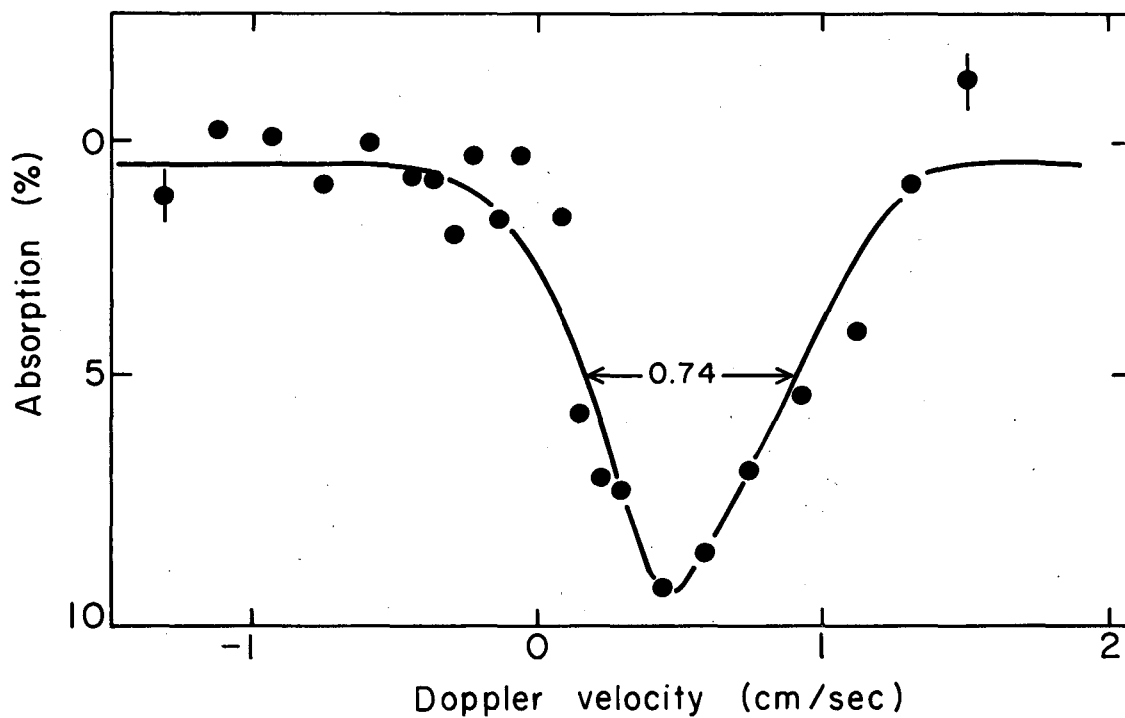
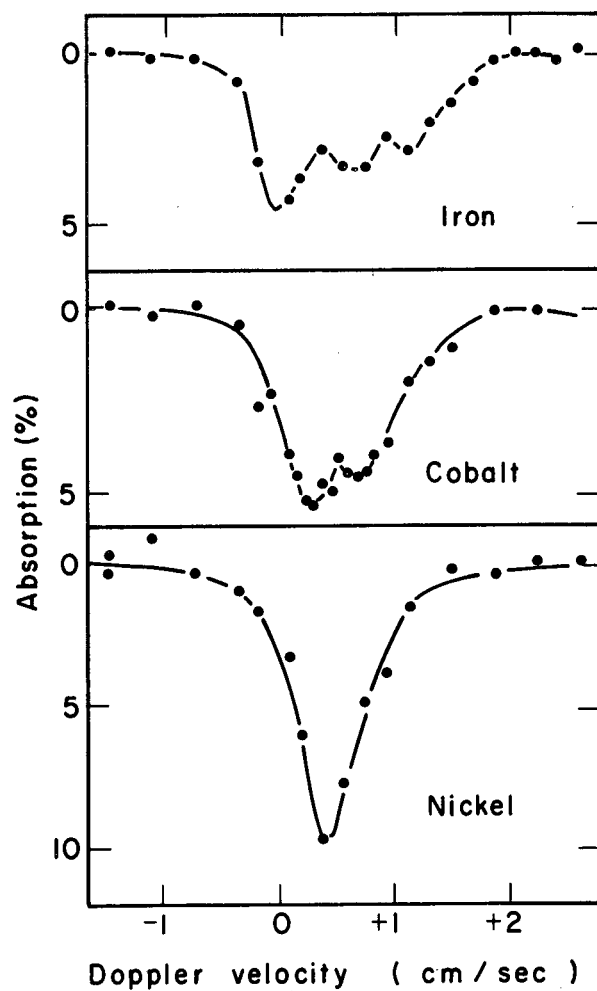


Fig. 4. Resonant absorption of 77-kev gamma ray of Au¹⁹⁷ obtained using 10-mil Au absorbers and sources of (a) Pt¹⁹⁷ in Pt metal and (b) Hg¹⁹⁷ in Pt metal. To obtain the percent absorption, correction factors of 1.52 and 1.95, respectively, were applied to the rough data.



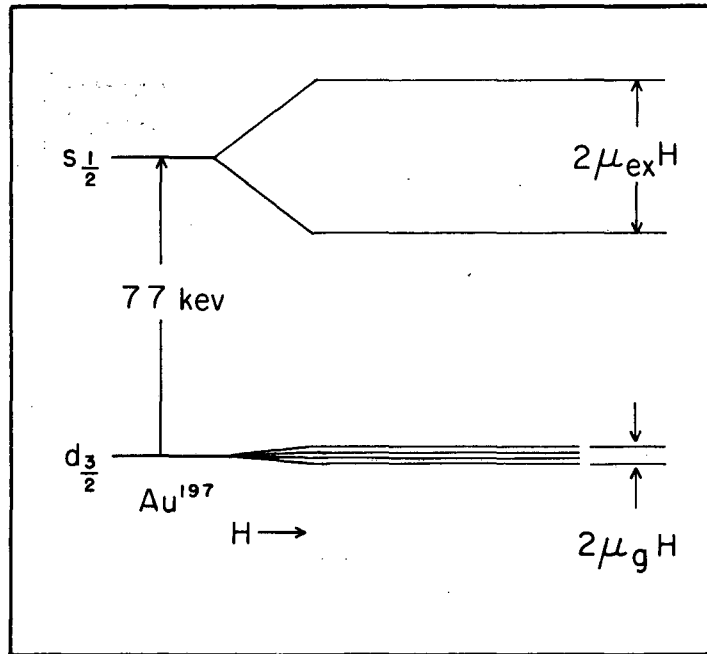
MU-22619-A

Fig. 5. Absorption curve for a source of Au¹⁹⁷ in stainless steel with a 10-mil Au absorber. A background correction factor of 2.5 was applied to the rough data to obtain percent absorption. The curve is not Lorentzian.



MII-22621

Fig. 6. Resonant-absorption curves for Au^{197} nuclei in iron, cobalt, and nickel lattices with a 10-mil Au absorber. The central minimum in iron is tentatively ascribed to Au atoms in improper sites. Percent absorption was calculated by applying a background correction factor of 1.50 to the raw data.



MU - 22620

Fig. 7. Expected Zeeman splitting for the 3 $s_{1/2}$ and 2 $d_{3/2}$ isomeric states of Au^{197} in a magnetic field H .

This report was prepared as an account of Government sponsored work. Neither the United States, nor the Commission, nor any person acting on behalf of the Commission:

- A. Makes any warranty or representation, expressed or implied, with respect to the accuracy, completeness, or usefulness of the information contained in this report, or that the use of any information, apparatus, method, or process disclosed in this report may not infringe privately owned rights; or
- B. Assumes any liabilities with respect to the use of, or for damages resulting from the use of any information, apparatus, method, or process disclosed in this report.

As used in the above, "person acting on behalf of the Commission" includes any employee or contractor of the Commission, or employee of such contractor, to the extent that such employee or contractor of the Commission, or employee of such contractor prepares, disseminates, or provides access to, any information pursuant to his employment or contract with the Commission, or his employment with such contractor.

